Ab Initio and Density Functional Theoretical Studies of Structures, Vibrational Spectra, and Dimerization Dynamics of Simple Transient Germenes†

Konstantin N. Kudin, John L. Margrave, and Valery N. Khabashesku*

Department of Chemistry, Rice University, Houston, Texas 77005-1892

Received: June 19, 1997; In Final Form: October 29, 1997

Structures and harmonic vibrational frequencies for several simple transient germenes, $H_2Ge{=}CH_2$ **(1)**, $MeHGe{=}CH_2$ **(2)**, $Me_2Ge{=}CH_2$ **(3)**, $FHGe{=}CH_2$ **(4)**, and $H_2Ge{=}CHF$ **(5)**, and their dimerization and transition state energies for the head-to-tail and head-to-head self-coupling have been calculated by ab initio HF 3-21G and 6-311G(d,p) and density functional theory B3LYP/6-311G(d,p) methods. The effect of substituents on the Ge═C bond lengths and bond orders, as well as frequencies and force constants of the Ge═C stretch, is predicted to be relatively small in germenes **1**−**3** and be substantially stronger in the F-substituted molecules **4** and **5**. Within the limits of the HF/3-21G method, the head-to-tail cyclodimerizations of all studied germenes **1**−**5** were found to be more exothermic than the head-to-head processes and to proceed with very low or zero barriers. This conclusion is confirmed for **1**−**4** by the higher level calculations with the 6-311G(d,p) basis set at HF and B3LYP levels, which in the case of **5** leads to the opposite result such as a substantial barrier for the head-to-tail dimerization and a lesser exothermicity of this process relative to the head-to-head one. The comparison of the HF/3-21G data available for the whole series of similarly substituted silenes with those calculated for **1**−**5** at the same level of theory indicate somewhat easier dimerization of germenes with respect to their double-bonded silicon analogues.

I. Introduction

Germenes,[1] $R_2Ge{=}CH_2$, possessing the organometallic chemical function >Ge═C<, are very reactive and considered to be prospective precursors for new polymers, ceramics, and other high-performance materials. The high reactivity of these species is particularly indicated by their extremely fast self-dimerization which precludes that germenes with small substituents (R) will exist as monomers under ambient conditions. Unlike stable germenes with bulky substituents,[1a,b] only indirect evidence for transient germenes has been accumulated until recently,[1c] and the ab initio studies of their reaction dynamics were limited to calculations[2] of the barrier heights for 1,2-H shift and reaction with water for the parent germene, $H_2Ge{=}CH_2$. This has been in contrast with the present state of research on simple transient silenes, $R_2Si{=}CR_2$, which have already been directly studied by spectroscopic techniques,[3a−c] and ab initio calculations at various levels of theory[4a,b] on the dimerization pathways for parent silene, $H_2Si{=}CH_2$,[5−9] have been caried out, including computational estimation of the substituent effects on the dimerization barriers.[10]

In our recent experimental work[11] we have succeeded in Fourier transform infrared spectroscopic characterization of the transient germene, $Me_2Ge{=}CH_2$. The detection of this species as a monomer was achieved due to its pyrolytic generation in the gas phase under pressures as low as 10^{-4} Torr and subsequent cryotrapping in argon or krypton at 12 K by the matrix isolation technique. Dimerization of this germene was observed in the gas phase already under pressures higher than 10^{-3} Torr or in an argon matrix at 35 K.[11b−d] These data seem to indicate a higher reactivity of germenes toward self-dimerization in comparison with their silicon analogues.

In an attempt to explain the experimental data and also for the purpose of comparison with the known 3-21G data on silenes we have carried out calculations both at the same level of theory and at the higher 6-311G(d,p) HF and density functional B3LYP levels of theory for dimerization of germenes with various substituents R, such as parent germene, $H_2Ge{=}CH_2$ **(1)**, 1-methyl-1-germene, $MeHGe{=}CH_2$ **(2)**, 1,1-dimethyl-1-germene, $Me_2Ge{=}CH_2$ **(3)**, 1-fluoro-1-germene, $FHGe{=}CH_2$ **(4)**, and 2-fluoro-1-germene, $H_2Ge{=}CHF$ **(5)**.

II. Computational Details

All calculations have been performed with the Gaussian 94 program[12] running on the NEC SX-3 supercomputer. First, optimized geometries and single-point energies were computed with the 3-21G basis set at the restricted Hartree−Fock level of theory in order to allow comparison with the data obtained for silenes at the same level of theory. Then the geometries were reoptimized with the 6-311G(d,p) basis set of triple-ζ quality both at the HF level and with the density functional theory (DFT)[13] B3LYP[14] method. The harmonic vibrational frequencies were calculated from the analytic second derivatives of the energy available at the HF and DFT procedure.

The search for the reaction transition state has been carried out according to the following procedure: (i) A variable *r* which represents a distance between the centers of two reacting molecules was created by adding a set of dummy atoms to the initial internal coordinate system. Thus a Z-matrix for the system under study was produced. (ii) Several values in the range of 4.5−2.5 Å were assigned to the *r* variable, and the energy of two approaching molecules for every fixed *r* value

† Dedicated to the 65th birthday of Professor Oleg M. Nefedov, Member and Vice-President of the Russian Academy of Sciences, and one of the major contributors to the chemistry of group 14 transient molecules.

S1089-5639(97)02006-9 CCC: $15.00
Published on Web 01/06/1998

TABLE 1: Optimized Parameters for Germene Monomers (1−5) for RHF/3-21G (1), RHF6-311G(d,p) (2), and B3LYP/6-311G (d,p) (3)

germene		total[a] and zero-point vibrational[b] energies	bond distances (Å)					valence angles (deg)				total net charge		dipole moment (D)
			Ge═C	Ge−H	Ge−R	C−H	C−R	HGeC	RGeC	HCGe	RCGe	Ge	C	
$H_2Ge{=}CH_2$	(1)		1.770	1.526		1.073		122.8		122.0		+0.774	−0.911	0.6078
	(2)	−2115.45337[a] 25.89[b]	1.763	1.520		1.075		122.8		121.8		+0.479	−0.543	0.8893
	(3)	−2117.47162[a] 24.27[b]	1.778	1.525		1.082		122.5		121.4		+0.371	−0.496	0.5908
$MeHGe{=}CH_2$	(1)		1.771	1.532	1.959	1.073[c]	1.074[d]	121.5	123.8	122.1[c]	122.0[d]	+1.006	−0.938	1.4332
	(2)	−2154.50729[a] 45.39[b]	1.764	1.526	1.951	1.075[c]	1.076[d]	121.1	124.8	121.7[c]	122.0[d]	+0.574	−0.580	1.7394
	(3)	−2156.80735[a] 42.85[b]	1.779	1.531	1.958	1.082[c]	1.083[d]	121.0	124.2	121.3[c]	121.7[d]	+0.472	−0.524	1.4617
$Me_2Ge{=}CH_2$	(1)		1.773		1.969	1.074			123.1	122.1		+1.260	−0.966	1.8621
	(2)	−2193.56095[a] 64.66[b]	1.765		1.954	1.076			123.2	121.9		+0.711	−0.610	2.1278
	(3)	−2196.14278[a] 61.05[b]	1.780		1.962	1.083			122.7	121.5		+0.615	−0.551	1.7996
$FHGe{=}CH_2$	(1)		1.754	1.516	1.696	1.072[c]	1.072[d]	130.0	121.1	121.0[c]	122.0[d]	+1.202	−1.006	1.9761
	(2)	−2214.36989[a] 22.62[b]	1.747	1.509	1.722	1.074[c]	1.073[d]	132.4	121.2	119.6[c]	122.3[d]	+0.973	−0.584	2.1304
	(3)	−2216.77298[a] 21.13[b]	1.764	1.518	1.755	1.081[c]	1.080[d]	133.2	120.0	119.3[c]	121.5[d]	+0.753	−0.519	1.9982
$H_2Ge{=}CHF$	(1)		1.780	1.519[c]	1.515[d]	1.070	1.378	117.9[c]	123.3[d]	125.7	121.9	+0.706	−0.291	2.3249
	(2)	−2214.31214[a] 21.47[b]	1.773	1.513[c]	1.513[d]	1.075	1.334	118.1[c]	123.2[d]	124.0	123.9	+0.380	−0.050	2.0969
	(3)	−2216.72032[a] 19.76[b]	1.794	1.518[c]	1.518[d]	1.085	1.353	117.9[c]	122.3[d]	124.3	123.4	+0.172	+0.036	1.6242

[a] Hartrees. [b] kcal/mol. [c] H *trans* to R. [d] H *cis* to R.

was minimizied by optimizing the other Z-matrix variables. The structure with the highest energy among these "semioptimized" structures was considered to be the closest one to the transition state and was used for further optimization. (iii) Final optimization of the transition state geometry involved calculations of the force constants for this "semioptimized" structure and then the internal Gaussian 94 procedure for the saddle point search. (iv) Calculations of the force constants and vibrational frequency analysis were also perfomed for the finally optimized transition state. The imaginary frequency corresponding to the normal mode of the molecular structure which represents the transition state was visualized by the Xmol program[15a] for SGI computers in order to make sure that the displacements that compose this mode point in the directions connecting the transition state with the minima of the structures of reactants and products. This additional step (iv) was absolutely necessary[4a,15b] to conclude that the saddle point found is a true transition state and it is consistent with the expected [2+2] cycloaddition chemistry of the studied germenes. The values of variables describing a four-membered ring were taken from the transition states for dimerization of parent germene **1**. Whenever possible, symmetry elements of the system were introduced into the Z-matrix. However, the symmetry constraints have been released and the optimization has been rerun in the cases when the symmetry introduction led to a structure with more than one imaginary frequency.

The force constants in the internal coordinates and the potential energy distributions (PED) for normal vibrational modes were computed with the REDONG program package.[16] The required Cartesian force constants and geometries for this procedure were taken directly from the Gaussian 94 output files.

III. Results and Discussion

Germene Monomers (1−5). *A. Molecular Geometries.* The HF/3-21G, HF/6-311G(d,p), and B3LYP/6-311G(d,p) optimized geometry parameters for germenes **1**−**5** with the substituents H, Me, and F at the germanium and H or F at carbon are given in Table 1. According to the energetic minima found at all three levels of theory, all of the germenes studied possess planar geometry in their singlet ground state. The Ge═C double-bond lengths were calculated to be in the range of 1.747−1.794 Å, depending on the substituent and the level of theory applied. They are considerably shorter than the Ge−C single bonds, e.g., in H_3GeCH_3, for which this bond length was calculated to be 1.976 Å at the RHF/3-21G(d) and 1.966 Å at the MP2/3-21G(d) levels.[17]

The methyl substituents at the germanium cause very little change in the Ge═C double-bond length in germenes **2** and **3** with regard to parent germene **1** while the F subsituent significantly shortens this bond in **4** and elongates it in **5**, where the F group is linked to the carbon atom. By analogy with the silenes,[7] the substituent effect on the length of the Ge═C double bond in the germenes can be explained in terms of the bond polarity. The Ge═C double bond is polarized, so that the Ge atom is positively charged and the C atom carries a negative charge, i.e., $Ge^{\delta+}{=}C^{\delta-}$. The electron-withdrawing substituents, in particular F, increase the positive charge at germanium (indicated in Table 1 by calculated total net charge) and thus the degree of the Ge═C bond ionicity. Therefore, this bond in **4**, where F is linked to germanium, is shorter than in **1**. When F is attached to the carbon atom, i.e., in **5**, the negative charge on this atom (Table 1) decreases due to withdrawing of most of the electron density to the F substituent. This reduces the Ge═C bond ionicity and lengthens this bond in **5** as compared to **1**. It also substantially increases the length of the dipole in **5**; therefore, the tendency for the dipole moment to increase in the direction from **1** to **5** is maintained, as shown in the Table 1, in spite of charge reduction both on the Ge and C atoms. The only exception from this tendency is found for the germene **5** at 6-311G(d,p) HF and B3LYP levels of theory, yielding lower values for the dipole moment in **5** than those in **3** and **4**.

TABLE 2: Vibrations of Germene, $H_2Ge{=}CH_2$ (1)

frequencies[a] no.	sym	HF/6-311G(d,p)	B3LYP/6-311G(d,p)	PED, %	assignment
1	b_1	420(28)[b]	332(18)	92 GeH_2 wag	GeH_2 wag
2	b_2	451(19)	451(13)	89 GeH_2 in-plane rock 11 CH_2 in-plane rock, op	GeH_2 in-plane rock
3	a_2	697(0)	701(0)	50 CH_2 twist, 50 GeH_2 twist	twisting mode
4	b_1	768(54)	730(54)	75 CH_2 wag, 25 GeH_2 wag	CH_2 wag
5	b_2	792(73)	802(55)	89 CH_2 in-plane rock, 11 GeH_2 in-plane rock, ip	CH_2 in-plane rock
6	a_1	814(24)	814(23)	96 Ge=C str	Ge=C str
7	a_1	851(20)	850(16)	87 GeH_2 scissor, 13 Ge=C str	GeH_2 scissor
8	a_1	1369(6)	1359(3)	100 CH_2 scissor	CH_2 scissor
9	a_1	2064(37)	2126(28)	100 GeH_2 sym str	GeH_2 sym str
10	b_2	2057(128)	2141(100)	100 GeH_2 asym str	GeH_2 asym str
11	a_1	2964(3)	3071(1)	100 CH_2 sym str	CH_2 sym str
12	b_2	3053(0)	3174(0)	100 CH_2 asym str	CH_2 asym str

[a] cm^{-1}. [b] Intensities in km/mol. op, out-of-phase. ip, in-phase.

TABLE 3: Vibrations of 1-Methyl-1-germene, $MeHGe{=}CH_2$ (2)

		frequencies[a]			
no.	sym	HF/6-311G(d,p)	B3LYP/6-311G(d,p)	PED, %	assignment
1	a″	110(0)[b]	102(0)	94 CH_3 torsion	CH_3 torsion
2	a′	178(6)	177(4)	100 CGeC in-plane bend	CGeC in-plane bend
3	a	299(8)	280(6)	45 GeH out-of-plane bend, 21 CH out-of-plane bend, ip; 28 CH_3 rock	GeH out-of-plane bend
4	a′	563(13)	572(13)	99 Ge−C str	Ge−C str
5	a″	593(9)	599(35)	64 CH out-of-plane bend, 34 GeH out-of-plane bend	CH out-of-plane bend
6	a′	613(30)	610(6)	69 GeH in-plane bend, 21 CH_2 in-plane rock, op	GeH in-plane bend
7	a″	729(44)	710(32)	94 CH_2 wag	CH_2 wag
8	a′	793(89)	804(68)	61 CH_2 in-plane rock, 21 GeH in-plane bend, 10 Ge=C str	CH_2 in-plane rock
9	a″	800(3)	809(0)	89 CH_3 rock, 10 CH out-of-plane bend	CH_3 rock
10	a′	825(17)	826(14)	98 Ge=C str	Ge=C str
11	a′	845(44)	857(44)	90 CH_3 rock	CH_3 rock
12	a′	1263(2)	1253(1)	98 CH_3 deform	CH_3 deform
13	a′	1368(7)	1357(4)	100 CH_2 scissor	CH_2 scissor
14	a″	1419(6)	1427(7)	97 CH_3 deform	CH_3 deform
15	a′	1423(6)	1432(7)	97 CH_3 deform	CH_3 deform
16	a′	2034(122)	2109(100)	100 GeH str	GeH str
17	a′	2856(11)	2967(6)	100 CH_3 str	CH_3 str
18	a″	2922(11)	3040(5)	100 CH_3 str	CH_3 str
19	a′	2937(8)	3056(4)	100 CH_3 str	CH_3 str
20	a′	2959(5)	3067(2)	100 CH_2 sym str	CH_2 sym str
21	a′	3047(2)	3168(1)	100 CH_2 asym str	CH_2 asym str

[a] cm^{-1}. [b] Intensities in km/mol.

B. Vibrational Spectra. The harmonic vibrational frequencies and infrared intensities predicted for the germenes **1**−**5**, as well as for the d_2-analogue of **3**, $Me_2Ge{=}CD_2$ **(6)**, both at HF/6-311G(d,p) and B3LYP/6-311G(d,p) levels of theory, are given in Tables 2−7. The only transient germene among **1**−**5**, for which a comparison of experimental and calculated frequencies can be made, is 1,1-dimethyl-1-germene **3**.[11] A very reasonable agreement between theory and experiment in the case of **3** has been achieved with the HF calculated harmonic frequencies scaled by a factor of 0.9. Even better agreement between measured frequencies and IR intensities and those calculated in this case was observed with the B3LYP frequencies scaled by a factor of 0.975 (Table 4). Given this demonstrated higher reliability of density functional B3LYP/6-311G(d,p) method in predicting vibrational spectra,[18] we have used the second derivatives' output values, obtained by this method, as a basis for calculations of internal-coordinate force constants and PED for each vibrational mode in **1**−**5** as well as in the deuterated derivative of **3**—$Me_2Ge{=}CD_2$ **(6)**. Thus, the description of predicted normal modes in **1**−**6** is additionally justified by taking into consideration the computed PED data.

Previous calculations of the vibrational spectra of parent germene **1** have been done with the 3-21G(d) basis set at the RHF, MP2, and MCSCF levels of theory.[17] They show a large discrepancy in the prediction of the location of the Ge=C stretch in **1**, e.g., 904 (RHF), 827 (MP2), and 785 (MCSCF) cm^{-1}. Our calculations, done with a larger basis set, 6-311G(d,p), yielded after the scaling procedure an identical value of 814

TABLE 4: Vibrations of 1,1-Dimethyl-1-germene, $Me_2Ge{=}CH_2$ (3)

		frequencies (cm^{-1})				
mode	sym	obsd[a]	HF/6-311G(d,p)	B3LYP/6-311G(d,p)	PED, %	assignment
1	a_2		107(0)[b]	104(0)[b]	100 CH_3 torsion, op	CH_3 torsion, op
2	b_1		116(0)	109(0)	76 CH_3 torsion, ip 24 $CGeC_2$ deformation	CH_3 torsion ip
3	b_1		145(1)	122(1)	99 $CGeC_2$ deformation	$CGeC_2$ deformation
4	a_1		166(0)	167(0)	100 GeC_2 scissor	GeC_2 scissor
5	b_2		184(13)	183(9)	100 GeC_2 rock	GeC_2 rock
6	a_2		525(0)	530(0)	100 CH_2 twist	CH_2 twist
7	a_1	576.0	543(6)	545(5)	100 Ge−C sym str	Ge−C sym str
8	b_2	580.1	576(23)	585(24)	100 Ge−C asym str	Ge−C asym str
9	b_1	596.0	664(81)	620(73)	98 CH_2 wag	CH_2 wag
10	b_2		684(3)	696(3)	78 CH_2 in-plane rock, 19 CH_3 rock	CH_2 in-plane rock
11	a_2		777(0)	791(0)	91 CH_3 rock	CH_3 rock
12	b_2	804.4	793(77)	804(63)	34 CH_3 rock, 59 CH_2 in-plane rock	CH_3 rock
13	b_1		798(1)	806(0)	92 CH_3 rock ip	CH_3 rock ip
14	a_1	818.8	816(4)	819(4)	99 Ge=C str	Ge=C str
15	a_1	847.3	840(70)	849(61)	74 CH_3 rock, op; 10 Ge=C stretch	CH_3 rock op
16	b_2	1241.7	1259(6)	1247(4)	100 CH_3 rock ip	CH_3 rock ip
17	a_1		1264(2)	1253(1)	100 CH_3 rock op	CH_3 rock op
18	a_1		1367(8)	1356(4)	100 CH_2 scissor	CH_2 scissor
19	a_2		1415(0)	1422(0)	88 CH_3 asym deformation	CH_3 asym deformation
20	b_2		1419(2)	1429(2)	99 CH_3 scissor op	CH_3 scissor op
21	b_1	1416.8	1423(7)	1433(13)	88 CH_3 scissor ip	CH_3 scissor ip
22	a_1	1451.7	1424(12)	1434(7)	96 CH_3 sym deformation	CH_3 sym deformation
23	b_2	2874.0	2850(17)	2962(11)	100 CH_3 asym str	CH_3 asym str
24	a_1		2851(11)	2963(7)	100 CH_3 sym str	CH_3 sym str
25	a_2		2912(0)	3032(0)	100 CH_3 asym str op	CH_3 asym str op
26	b_1	2927.9	2913(27)	3032(14)	100 CH_3 asym str ip	CH_3 asym str ip

[a] Reference 11. [b] Intensities in km/mol.

cm^{-1} for this mode both at HF and B3LYP levels of theory (Table 2). Such excellent agreement found for this particular mode as well as the very good agreement noticed for the other frequencies lying below 2000 cm^{-1} shows that the frequencies and IR intensities calculated at these higher levels of theory are more reliable and thus can be of valuable assistance for the experimental IR identification of transient germene **1**.

The frequency of the Ge=C stretch is predicted to increase only slightly (by 2−12 cm^{-1}) in the direction **1** < **2** < **3** under the influence of Me substituents (Tables 2−4). Meanwhile, the F substituents cause more significant shifts of the Ge=C stretch in **4** and **5** as compared with that in **1**, increasing this frequency by 28−31 cm^{-1} in 1-fluoro-substituted germene **4** (Table 6) and decreasing it by 49−52 cm^{-1} in 2-fluoro-1-germene **5** (Table 7). The substitution of the $=CH_2$ group in **3** by the $=CD_2$ moiety is predicted to cause even a larger shift (by 56−58 cm^{-1}) of the Ge=C stretch toward a lower frequency in $Me_2Ge{=}CD_2$ (**6**) (Table 5) with respect to $Me_2Ge{=}CH_2$ (**3**) (Table 4).

The calculated PED values show no or some degree of coupling of the Ge=C stretching vibration with the other modes of the same symmetry in **1**−**6**. The Ge=C stretching mode in **4** is predicted to be virtually pure, while this mode is coupled to some degree with the GeH_2 scissoring motion in **1**, CH_2 rocking and GeH bending in-plane modes in **2**, CH_3 rocking in **3**, GeH in-plane bending motion in **5**, and CD_2 scissor in **6** (Tables 2−7).

The computed infrared intensities at both HF and DFT levels of theory predict the Ge=C stretching vibration to show either medium or low band intensity in the IR spectra with the highest oscillator stength calculated for this mode in **1** (23−24 km/mol) and the lowest in **3** (4 km/mol), as given in Tables 2 and 4, respectively. The latter prediction agrees well with the recent experimental observation of the Ge=C stretch in **3** as a very low intensity band at 818.8 cm^{-1} in the argon matrix FTIR spectrum.[11d]

The frequency of the "olefinic" $=CH_2$ wagging mode is predicted to be significantly dependent on the nature of the substituent attached to the Ge end of the Ge=C bond. This frequency tends to shift from 730 to 768 cm^{-1} to lower energies (620−664 cm^{-1}) in the following direction: **1** > **2** > **4** > **3** (Tables 2−4, 6). The CH_2 wagging mode is predicted to exhibit a high intensity in the IR spectra of germenes **1**−**5**, which, in particular, agrees well with the observation of a high-intensity band of this mode at 596.0 cm^{-1} in the FTIR spectrum of **3**.[11] The high intensity is also expected for the $=CD_2$ wagging mode in **6** (Table 5), which in this molecule is shifted to lower frequencies by 135−138 cm^{-1} as compared to that in **3** (Table 4).

C. The Ge=C Force Constants and Bond Orders. The force constants in internal coordinates for the Ge=C bonds in **1**−**5**, calculated with the use of the REDONG program package for all sets of scaled vibrational frequencies at HF and density functional B3LYP levels of theory, and the Ge=C bond orders, estimated according to Siebert's rule[19] with regard to a force constant of the Ge−C single bond in CH_3GeH_3 (2.72 mdyn/Å), are given in Table 8. The Ge=C force constants in **1**−**3** are calculated to be very close (4.74−4.79 mdyn/Å). However, they differ significantly in **4** and **5**, where the largest value among the **1**−**5** series is computed for 1-fluoro-substituted germene **4** (4.94−4.99 mdyn/Å) and the lowest for the 2-fluoro derivative **5** (4.50−4.65 mdyn/Å). An overall change in the Ge=C force constants in **1**−**5** follows the trend **4** > **1** > **2** ∼ **3** > **5**.

TABLE 5: Vibrations of 1,1-Dimethyl-1-germene-d_2, $Me_2Ge{=}CD_2$ (6)

		frequencies (cm^{-1})			
mode	sym	HF/6-311G(d,p)	B3LYP/6-311G(d,p)	PED, %	assignment
1	a_2	108(0)[a]	105(0)[a]	100 CH_3 torsion, op	CH_3 torsion, op
2	b_1	116(0)	109(0)	47 CH_3 torsion, ip; 42 $CGeC_2$ deform deform	CH_3 torsion ip
3	b_1	143(1)	122(0)	99 $CGeC_2$ deform	$CGeC_2$ deform
4	a_1	166(0)	166(0)	99 GeC_2 scissor	GeC_2 scissor
5	b_2	166(9)	167(6)	100 GeC_2 rock	GeC_2 rock
6	a_2	385(0)	387(0)	100 CD_2 twist	CD_2 twist
7	b_1	526(56)	485(47)	97 CD_2 wag	CD_2 wag
8	a_1	542(5)	544(5)	100 Ge−C sym str	Ge−C sym str
9	b_2	556(11)	565(7)	97 CD_2 in-plane rock	CD_2 in-plane rock
10	b_2	578(37)	588(37)	99 Ge−C asym str	Ge−C asym str
11	a_1	740(15)	741(11)	95 Ge=C str	Ge=C str
12	b_2	759(48)	771(38)	87 CH_3 rock	CH_3 rock
13	a_2	759(0)	775(0)	96 CH_3 rock	CH_3 rock
14	b_1	779(3)	793(5)	95 CH_3 rock	CH_3 rock
15	a_1	836(46)	846(46)	84 CH_3 rock	CH_3 rock
16	a_1	1060(21)	1052(13)	84 CD_2 scissor, 16 Ge=C str	CD_2 scissor
17	b_2	1259(5)	1247(4)	100 CH_3 deform rock	CH_3 deform rock
18	a_1	1265(2)	1254(1)	100 CH_3 deform rock	CH_3 deform rock
19	a_2	1415(0)	1423(0)	88 CH_3 asym deform	CH_3 asym deform
20	b_2	1419(2)	1429(2)	93 CH_3 scissor op	CH_3 scissor op
21	b_1	1424(6)	1434(13)	88 CH_3 scissor ip	CH_3 scissor ip
22	a_1	1424(12)	1434(7)	92 CH_3 sym deform	CH_3 sym deform
23	a_1	2145(1)	2221(0)	100=CD_2 sym str	=CD_2 sym str
24	b_2	2263(0)	2355(0)	100=CD_2 asym str	=CD_2 asym str
25	b_2	2850(17)	2962(11)	100 CH_3 asym str	CH_3 asym str
26	a_1	2852(11)	2963(7)	100 CH_3 sym str	CH_3 asym str
27	a_2	2913(0)	3033(0)	100 CH_3 asym str op	CH_3 asym str op
28	b_1	2914(27)	3033(14)	100 CH_3 asym str ip	CH_3 sym str ip
29	b_2	2933(9)	3053(5)	95 CH_3 asym str in-plane	CH_3 asym str in-plane
30	a_1	2934(11)	3053(7)	95 CH_3 sym str in-plane	CH_3 sym str in-plane

[a] Intensity, in km/mol. ip, in-phase. op, out-of-phase. str, stretch.

TABLE 6: Vibrations of 1-Fluoro-1-germene, $FHGe{=}CH_2$ (4)

		frequencies (cm^{-1})			
no.	sym	HF/6-311G(d,p)	B3LYP/6-311G(d,p)	PED, %	assignment
1	a′	205(19)[a]	207(12)[a]	100 GeF in-plane bend	GeF in-plane bend
2	a″	295(21)	233(16)	89 GeH out-of-plane bend, 11 CH out-of-plane bend, ip	GeH out-of-plane bend
3	a″	563(4)	543(5)	99 CH out-of-plane bend	CH out-of-plane bend
4	a′	642(74)	651(56)	82 Ge−F str, 14 CH_2 in-plane rock	Ge−F str
5	a″	678(53)	680(46)	78 CH_2 wag, 22 GeH out-of-plane bend	CH_2 wag
6	a′	713(52)	680(31)	66 CH_2 in-plane rock, 21 GeH in-plane bend, op	CH_2 in-plane rock
7	a′	794(57)	805(49)	68 GeH in-plane bend, 32 CH_2 in-plane rock, ip	GeH in-plane bend
8	a′	845(18)	842(11)	100 Ge=C str	Ge=C str
9	a′	1350(9)	1332(5)	100 CH_2 scissor	CH_2 scissor
10	a′	2114(41)	2162(34)	100 GeH str	GeH str
11	a′	2972(0)	3082(1)	100 CH_2 sym str	CH_2 sym str
12	a′	3070(1)	3195(1)	100 CH_2 asym str	CH_2 asym str

[a] Intensities in km/mol. ip, in-phase. op, out-of-phase.

The Ge=C bond orders change in the same direction. The highest value is predicted for the Ge=C bond in **4** (1.62−1.65) and the lowest for that in **5** (1.51−1.55). This is in line with the changes in Ge=C bond lengths within the **1**−**5** series, already discussed above, and also suggests that the π-bond is probably the strongest in **4** and the weakest in the germene **5**.

Dimerization Reaction of Germenes 1−5. It was expected that the calculated structural parameters, dipole moments and the total net charges on the Ge and C atoms in the monomers **1**−**5** should affect their dimerization pathways, transition state energies, and the exothermicity of these reactions that can proceed either in a head-to-tail or a head-to-head fashion.

A. Head-to-Tail Dimerization. We have studied the concerted 2S + 2S mechanism for the head-to-tail dimerization of **1**−**5**, which is symmetry allowed for the molecules with polarized double bonds, to allow a comparison with the available data on the same dimerization pathway computed for a series of substituted silenes.[10] A theoretical investigation of a non-

TABLE 7: Vibrations of 2-Fluoro-1-germene, $H_2Ge{=}CHF$ (5)

		frequencies (cm^{-1})			
no.	sym	HF/6-311G(d,p)	B3LYP/6-311G(d,p)	PED, %	assignment
1	a″	257(4)[a]	106(2)[a]	35 GeH_2 wag	GeH_2 wag
2	a′	283(4)	260(3)	98 CF in-plane bend	CF in-plane bend
3	a″	464(0)	461(0)	96 GeH_2 twist	GeH_2 twist
4	a′	521(55)	522(38)	87 GeH_2 in-plane rock 11 Ge=C str	GeH_2 in-plane rock
5	a″	762(24)	727(29)	90 CH out-of-plane bend, 10 GeH out-of-plane bend, ip	CH out-of-plane bend
6	a′	765(17)	762(12)	86 Ge=C str, 10 GeH in-plane bend	Ge=C str
7	a′	811(14)	810(16)	100 GeH_2 scissor	GeH_2 scissor
8	a′	1123(309)	1125(222)	98 GeH_2 scissor	GeH_2 scissor
9	a′	1336(75)	1322(50)	98 CH in-plane bend	CH in-plane bend
10	a′	2089(19)	2152(11)	100 GeH_2 sym str	GeH_2 sym str
11	a′	2092(89)	2178(68)	100 GeH_2 asym str	GeH_2 asym str
12	a′	3015(4)	3088(4)	100 C−H str	C−H str

[a] Intensities in km/mol.

TABLE 8: Calculated Ge=C Force Constants (*K*) and Estimated Ge=C Bond Orders (*N*) in Transient Germenes 1−5

	$H_2Ge{=}CH_2$ (**1**)	$MeHGe{=}CH_2$ (**2**)	$Me_2Ge{=}CH_2$ (**3**)	$HFGe{=}CH_2$ (**4**)	$H_2Ge{=}CHF$ (**5**)
			HF/6-311G(d,p)		
K(Ge=C)[a]	4.79	4.75	4.75	4.99	4.65
N (Ge=C)	1.58	1.57	1.57	1.64	1.55
			B3LYP/6-311G(d,p)		
K (Ge=C)[a]	4.79	4.75	4.74	4.94	4.50
N (Ge=C)	1.58	1.57	1.57	1.62	1.51

[a] mdyn/Å.

concerted dimerization mechainsm has also recently been done;[9] however, in the case of silenes it was limited only to a parent molecule, $H_2Si{=}CH_2$.

The head-to-tail dimerization-cycloaddition of germene monomers yields 1,3-digermacyclobutanes according to eq 1:

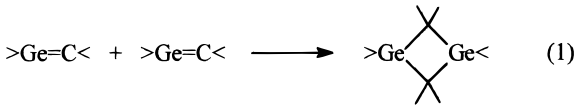

(1)

The search for the transition states in the case of **1**−**5**, described in the Computational Details section, was performed in a way opposite to a procedure used by Seidl et al.[8] for the location of stationary points on the potential energy surface for a similar dimerization path of parent silene. The structures found have only one imaginary vibrational frequency at each level of theory, and thus they represent true transition states. The dimerization and transition state energies for this reaction path are given in Table 9, and the optimized geometries of the head-to-tail dimerization transition states found for the germenes **1**−**3** and **5** at all three levels of theory are shown in Chart 1.

For all of the reacting germenes the calculations yield a planar rombic geometry for the CGeCGe unit of the transition state. A comparison of the Ge=C distances for monomers **1**−**3** and **5** from Table 1 with the r_1(Ge−C) distances in the head-to-tail dimerization transition states from Chart 1 reveals only a slight elongation of the latter by an average 0.018 Å at HF/3-21G, 0.024 Å at HF/6-311G(d,p), and 0.045 Å at B3LYP/6-311G-(d,p) levels of theory. This indicates the conservation of the sp^2 configuration for the germanium and carbon in the transition state for the head-to-tail dimerization, meaning that the transition states found closely resemble the structures of reacting germenes.

The r_2 distance between Ge and C atoms varies depending on the substituent nature and position, and probably Ge=C bond polarity in the reactants, i.e., r_2 substantially increases from **1** to **3** with the accumulation of the number of methyl groups at germanium and decreases in **5** where F is attached to carbon. Since the steric effect of a methyl group at distances larger than 3.0 Å should be quite small, the calculated increase in r_2 for **1**−**3** may be also related to the increasing Ge=C bond polarity on going from **1** to **3**, resulting in an earlier transition state, i.e., longer r_2, which is in accord with the transition state energy ($\Delta E^{\ddagger}$) decrease in the direction **1** > **2** > **3** (Table 9). The *cis* or *trans* position of methyl substituents insignificantly affects the distance r_2 for the dimerization transition state of germene **2** at all three levels of theory. Meanwhile, in the case of F-substituted germene **5** the r_2 values differ significantly (by 0.153 Å) for the *cis* and *trans* isomers at the lowest (HF/3-21G) level of theory applied; however, they are found to be almost identical at the higher levels of calculation.

Three different types of reaction profiles have been found for the head-to-tail dimerization of germenes **1**−**5**. They are shown in Figure 1 as A, B, and C. The energy level of the monomers in all reaction passages is taken as zero. The profiles A and B pass through the energy minima due to formation of weak van der Waals complexes; then they climb to the top of an energy hill where a saddle point characterizing a particular transition state is located. Finally, these profiles (as well as the profile C) end up with global energy minima of reaction products−1,3-dimers, indicating the highly exothermic nature

TABLE 9: Summary of Transition State ($\Delta E^{\ddagger}$ and $\Delta H^{\ddagger}$) and Dimerization (ΔE and ΔH) Energies, kcal/mol, for RHF/3-21G (1), RHF/6-311G(d,p) (2), and Becke3LYP/6-311G(d,p) (3)

		head-to-tail				head-to-head			
germene (**1**−**5**)		$\Delta E^{\ddagger}$	$\Delta H^{\ddagger}$	ΔE	ΔH	$\Delta E^{\ddagger}$	$\Delta H^{\ddagger}$	ΔE	ΔH
$H_2Ge{=}CH_2$	(1)	4.9 (8.5)[a]	6.0	−98.5	−95.1	32.5	32.9	−79.8	−75.3
	(2)	5.3	6.4	−78.7	−75.3	34.0	34.4	−76.1	−71.6
	(3)	2.5 [3.8][b]	3.6 [5.2][b]	−68.7	−65.3	20.3	20.7	−68.5	−64.0
$MeHGe{=}CH_2$	(1)	0.4 (13.0)	0.9	−98.9	−96.3	33.4	33.5	−79.1	−75.3
(*trans*)	(2)	2.6	3.1	−78.3	−75.7	36.7	36.8	−74.2	−70.4
	(3)	0.4	0.9	−68.5	−65.9	21.6	21.7	−67.2	−63.4
$MeHGe{=}CH_2$	(1)	0.5	1.0	−98.9	−96.3	33.5	33.6	−79.3	−75.5
(*cis*)	(2)	2.7	3.2	−78.2	−75.6	36.8	36.9	−73.8	−70.0
	(3)	0.6	1.1	−68.4	−65.8	21.7	21.8	−66.8	−63.0
$Me_2Ge{=}CH_2$	(1)	−3.8	−3.6	−99.4	−97.4	33.9	33.7	−79.0	−75.7
	(2)	0.4	0.6	−77.9	−75.9	39.3	39.1	−71.8	−68.5
	(3)	−1.2	−1.0	−68.4	−66.4	22.8	22.6	−65.3	−62.0
$FHGe{=}CH_2$	(1)	no TS (−4.8)		−123.0	−120.0	26.6	26.4	−93.3	−89.1
(*trans*)	(2)	no TS		−94.0	−91.0	27.9	27.7	−86.1	−81.9
	(3)	no TS		−82.8	−79.8	13.8	13.6	−78.9	−74.7
$FHGe{=}CH_2$	(1)	no TS		−122.5	−119.5	26.8	26.6	−92.0	−87.8
(*cis*)	(2)	no TS		−93.3	−90.3	28.8	28.6	−84.9	−80.7
	(3)	no TS		−82.2	−79.2	14.6	14.4	−77.7	−73.5
$H_2Ge{=}CHF$	(1)	−3.7	−3.1	−95.9	−93.1	18.7	18.9	−97.8	−93.9
(*trans*)	(2)	11.6	12.2	−77.1	−74.3	20.2	20.4	−91.6	−87.7
	(3)	<5.8	<6.4	−64.9	−62.1	not found		−77.6	−73.7
$H_2Ge{=}CHF$	(1)	11.7 (15.5)	12.3	−94.7	−91.9	13.9	14.1	−93.1	−89.1
(*cis*)	(2)	11.7	12.3	−76.4	−73.6	21.8	22.0	−90.8	−86.8
	(3)	<6.2	<6.8	−64.3	−61.5	not found		−77.3	−73.3

[a] The HF/3-21G transition state energies for the substituted silenes from ref 10 are shown in parentheses. [b] CCSD/DZ+d transition state energies for the dimerization of parent silene from ref 8 are shown in brackets.

CHART 1: Optimized Geometries for the Head-to-Tail Dimerization Transition States for RHF/3-21G (1), RHF/6-311G(d,p) (2), and Becke3LYP/6-311G(d,p) (3)

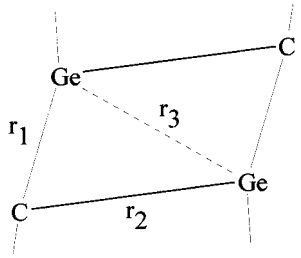

		r_1, Å	r_2, Å	r_3, Å	GeCGe, deg
$H_2Ge{=}CH_2$	(1)	1.789	3.037	3.225	79.3
	(2)	1.787	2.998	3.033	73.8
	(3)	1.821	2.923	2.750	66.1
$MeHGe{=}CH_2$	(1)	1.789	3.093	3.283	79.7
trans	(2)	1.788	3.040	3.103	75.0
	(3)	1.818	2.982	2.810	66.6
$MeHGe{=}CH_2$	(1)	1.789	3.080	3.282	79.7
cis	(2)	1.788	3.036	3.102	75.1
	(3)	1.818	2.977	2.810	66.7
$Me_2Ge{=}CH_2$	(1)	1.789	3.171	3.356	79.9
	(2)	1.789	3.085	3.179	76.3
	(3)	1.815	3.050	2.892	67.5
$H_2Ge{=}CHF$	(1)	1.779	3.044	3.666	95.3
trans	(2)	1.802	2.868	2.854	71.2
	(3)	1.863	2.760	2.570	64.1
$H_2Ge{=}CHF$	(1)	1.800	2.891	3.153	80.9
cis	(2)	1.803	2.854	2.849	71.4
	(3)	1.862	2.756	2.574	64.4

of these reactions. The dimerizations of germenes **1**, **2**, and **5** (toward *cis*-1,3-dimer) proceed along the A type profiles with the transition states lying above the energy level of monomers and thus are calculated to have positive energy ($\Delta E^{\ddagger}$) values at all three levels of theory (Table 9). At the same time, the predicted dimerization profiles for **3** and **5** (to form the *trans*-1,3-dimer) show a dependence on the calculation method used. The A type profiles are predicted for **3** and **5** at HF/6-311G-(d,p) as well as for **5** also at the B3LYP level of theory, while the B type profiles with the transition states lying below the monomers in terms of energy, so that the $\Delta E^{\ddagger}$ values are negative, were computed for **3** with HF/3-21G and B3LYP methods and also found for **5**, but only at the lowest level of theory.

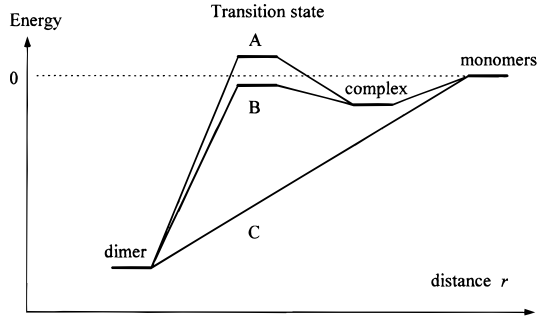

Figure 1. Three types (A, B, and C) of reaction profiles predicted for the head-to-tail dimerization of germenes 1−5.

No transition states were located for the dimerizations of 1-fluoro-substituted germene **4** toward both the *cis*- and *trans*-1,3-dimer. Point-by-point calculations at all three theory levels have yielded a C type profile for the reactions that are likely to proceed with no energy barrier.

The calculated transition state energies ($\Delta E^{\ddagger}$) for the head-to-tail dimerization are decreasing for the germenes **1**−**3** in the order **1** < **2** < **3** (Table 9) in accord with the increase of total net charges on the germanium and carbon atoms in the following order **3** > **2** > **1** (Table 1). At the lowest level of theory (HF/3-21G) these data predict a higher kinetic stability for the parent germene **1** with respect to methyl-substituted **2** and **3** and fluoro-substituted germenes **4** and **5**. This is in line with the relative kinetic stability of the similarly substituted silenes, assumed from their HF/3-21G dimerization barrier heights calculated by

Morokuma[10] and shown in Table 9 in parentheses. The highest barrier was predicted for 2-fluorosilene (15.5 kcal/mol), while the lowest was for the 1-fluoro derivative (−4.8 kcal/mol), in full agreement with the net charge distribution on the Si and C atoms in these molecules. From this point of view, one would expect the highest $\Delta E^{\ddagger}$ value for 2-fluorogermene **5** too, since the positive and negative charges on Ge and C atoms are the smallest (Table 1) among studied germenes. Indeed, within the limits of the HF/3-21G method it was found to be the case for the *cis* coupling of 5, while the *trans* dimerization is predicted to proceed through a negative barrier (profile B).

The higher level calculations, performed with the extended basis set augmented with polarization functions on germanium, carbon, and hydrogen, 6-311G(d,p), at the HF and B3LYP levels of theory, confirm the conclusions made for germenes **1**−**3** with the lower level computation. On the contrary, for the head-to-tail dimerization of **5** these calculations yield notable barriers of 11.6−11.7 kcal/mol and 5.8−6.2 kcal/mol with HF and B3LYP, respectively. They also predict a practically equal likelihood for the *cis* and *trans* dimerization pathways of **5**. The latter conclusion is found to be true for the dimerization of germene **2** as well, at all three levels of theory used.

In accord with the reactivity of 1-fluoro-1-silene, for which the HF/3-21G head-to-tail dimerization barrier was found to be −4.8 kcal/mol,[10] the germene analogue **4** is predicted at all three levels of theory to react without a barrier both in the *cis* and *trans* fashion. This very high reactivity of **4** seems to be consistent with the high degree of polarization of the Ge═C bond in this molecule as reflected by the calculated large net charges on Ge and C atoms (Table 1).

The energies ΔE (Table 9), calculated at the HF/3-21G level of theory and usually yielding somewhat overestimated values, show high exothermicities (above 94 kcal/mol) for all head-to-tail dimerization reactions of germenes **1**−**5**, with the dimerization of **4** the most exothermic (123 kcal/mol) in particular. Thus, these reactions have been predicted to be even more exothermic than those of substituted silenes, e.g., their HF/3-21G dimerization energies were calculated to range within 70−84 kcal/mol.[7] The higher level calculations are giving lower ΔE values, by 10−20 and 30−40 kcal/mol with 6-311G(d,p) HF and B3LYP, respectively, than those computed with 3-21G. The B3LYP ΔE value for the dimerization of the parent germene **1** (68.7 kcal/mol) is found to be lower than the 2S + 2S head-to-tail dimerization energy for the parent silene (83.1 kcal/mol) recently calculated with the CCSD/DZ+d method.[8] The higher quality computational data are not currently available for the substituted silenes, although the comparison made above for the parent silene/germene pair allows one to assume that they will likely predict lower dimerization energies for the substituted germenes relative to their silicon analogues. In a meantime, the calculated dimerization barriers suggest a higher reactivity of germenes with respect to silenes toward a head-to-tail self-dimerization.

B. Head-to-Head Dimerization. Our approach to the search for the transition state in this case was similar to that discussed above for the head-to-tail dimerization reaction. This self-dimerization reaction of two germenes should yield 1,2-digermacyclobutanes, according to eq 2.

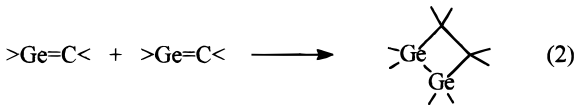

In contrast to the recent computational studies on the head-to-head dimerization of parent silene, where no closed-shell SCF stationary points have been located, we found the transition states for all reacting germenes at all three levels of theory used with the exception of **5** at the B3LYP level. Since this type of dimerization was experimentally observed only for a few several silenes, such as $(Me_3Si)_2Si{=}CR(OSiMe_3)$,[10] and not for the germenes, the calculational data on the transition states and dimerization energies would seem to be valuable in developing an insight into the head-to-head coupling mechanism of **1**−**5**.

CHART 2: Optimized Geometries for the Head-to-Head Dimerization Transition States for RHF/3-21G (1), RHF/6-311G(d,p) (2), and Becke3LYP/6-311G(d,p) (3)

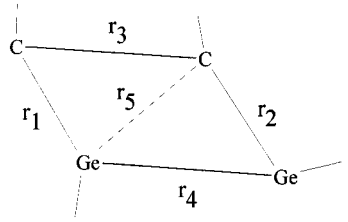

		r_1, Å	r_2, Å	r_3, Å	r_4, Å	r_5, Å	GeCCGe, deg
$H_2Ge{=}CH_2$	(1)	1.788	1.963	2.666	3.346	2.959	0
	(2)	1.796	1.954	2.772	3.119	2.862	0
	(3)	1.884	1.971	2.678	2.804	2.249	0
$MeHGe{=}CH_2$	(1)	1.790	1.965	2.598	3.524	3.059	2.5
trans	(2)	1.804	1.935	2.772	3.059	2.837	1.8
	(3)	1.888	1.952	2.687	2.785	2.277	0.2
$MeHGe{=}CH_2$	(1)	1.790	1.969	2.611	3.494	3.072	9.2
cis	(2)	1.803	1.936	2.770	3.069	2.843	6.8
	(3)	1.888	1.951	2.690	2.786	2.279	2.8
$Me_2Ge{=}CH_2$	(1)	1.795	1.963	2.568	3.582	3.160	0
	(2)	1.811	1.923	2.773	3.019	2.825	0
	(3)	1.891	1.939	2.704	2.784	2.302	0
$FHGe{=}CH_2$	(1)	1.772	1.954	2.814	3.233	3.076	5.2
trans	(2)	1.775	1.949	2.962	3.088	3.080	3.0
	(3)	1.861	1.923	2.851	2.701	2.315	6.3
$FHGe{=}CH_2$	(1)	1.771	1.954	2.821	3.241	3.078	8.1
cis	(2)	1.773	1.953	2.955	2.139	3.107	10.3
	(3)	1.857	1.922	2.877	2.733	2.316	20.4
$H_2Ge{=}CHF$	(1)	1.790	2.033	2.588	3.405	3.177	5.0‘
trans	(2)	1.794	2.046	2.757	3.151	3.048	6.1
$H_2Ge{=}CHF$	(1)	1.815	1.932	3.208	2.954	3.639	24.2
cis	(2)	1.796	2.057	2.779	3.130	3.031	3.1
	(3)						

A sketch and the HF/3-21G, HF/6-311G(d,p) and B3LYP/6-311G(d,p) optimized geometry parameters for the transition states are shown in Chart 2. In the transition states for the dimerization of **1** and **3** the GeCCGe unit is lying in one plane, while it is slightly or significantly distorted from the planar geometry in the case of the other germenes, **2**, **4**, and **5**. It is important to note the difference in the geometrical configurations of the two germene molecules in the transition state. This difference is indicated by the r_1 and r_2 distances and valence angles for the Ge and C atoms. The r_1 distances (1.771−1.891 at HF/3-21G, 1.773−1.811 Å at HF/6-311G(d,p), and 1.857−1.891 Å at B3LYP/6-311G(d,p)) that are about the same or slightly longer than the Ge═C double bonds in the germenes **1**−**5** (Table 1**)** and the sp^2 valence angles at the Ge and C atoms bonded by the r_1 linkage show the conservation of germene geometry for one of the reacting molecules. As for the other molecule, the r_2 distances (1.932−2.033 Å at HF/3-21G, 1.923−2.057 Å at HF/6-311G(d,p), and 1.922−1.971 Å at B3LYP/6-311G(d,p)) are calculated to be very close to the single Ge−C bond lengths[17] and the valence angles to retain the sp^2 configuration at carbon and to invert into approximately sp^3 at the germanium (angles within 95−105°). This geometry almost resembles the structure of an open-shell triplet or singlet excited

states of the parent germene[17] with the only difference being that it is not twisted. Since in our calculations a singlet structure for the reacting germene **1**−**5** has been set in advance, we believe that the head-to-head dimerization transition state has some singlet biradical character.

During the further reaction step toward formation of 1,2-cyclodimers (eq 2) this transition state very likely converts into 1,4-biradical intermediates by analogy with the head-to-head dimerization of silenes $(Me_3Si)_2Si{=}CR(OSiMe_3)$, for which those radicals have been detected by electron spin resonance spectroscopy.[20a,b] Several open-shell C−C and Si−Si broken diradical structures have been located on the potential energy surface for the head-to-head dimerization of silene.[8] On this basis a conclusion was made that this reaction should pass through a multistep process involving diradical intermediates. To justify the feasibility of a similar mechanism for the head-to-head dimerization of germenes **1**−**5**, the further high-level computational studies on the consecutive steps of these reactions have to be done.

Since the transition state of the head-to-head dimerization, shown in Chart 2, inevitably requires breaking of the Ge=C π-bond, the barriers $\Delta E^{\ddagger}$ are overall expected to be higher than those for the head-to-tail coupling. The calculated HF 3-21G and 6-311G(d,p) $\Delta E^{\ddagger}$ barriers (Table 2) for the germenes **1**−**3**, ranging from 32.5 to 39.1 kcal/mol, are the highest. They are close to the π-bond strength in germene **1** which is estimated as about 31 kcal/mol by the direct MCSCF energy difference between planar π-bonded and perpendicular biradical structures and as 33 kcal/mol from a thermochemical cycle computational investigation.[17] The lowest barriers were computed for the *cis* and *trans* coupling of the germene **5**, where the Ge=C π-bond is expected to be the weakest one, the charge distribution is calculated to be the most balanced one among the **1**−**5** series, and the F substituents provide an additional stabilization to a biradical-like transition state.

At HF/3-21G level of theory all head-to-head dimerization reactions were calculated to be much less exothermic (by ∼20−30 kcal/mol) than the head-to-tail coupling with the exception of **5** which reacts in both cases with about the same dimerization energy. The higher level 6-311G(d,p) HF and B3LYP calculations yield persistently lower and closer ΔE values for both dimerization pathways. They, in particular, predict the head-to-head dimerization of **1**−**4** still to be less exothermic than the head-to-tail coupling, however, by only 0.2−8.4 kcal/mol. In the case of the germene **5** these calculations even yield a higher exothermicity (by 12.7−14.4 kcal/mol) for the head-to-head self-dimerization reaction than that for the head-to-head one. This latter case is very likely controlled by the electron-withdrawing nature of the F substituent similar to the effect of the $OSiMe_3$ group at carbon on the dimerization path of silenes.[20]

IV. Conclusion

According to the lowest level of calculations used in the present study, HF 3-21G, the head-to-tail cyclodimerization of the germenes **1**−**5**, yielding 1,3-digermacyclobutanes, is more exothermic than the head-to-head coupling to form 1,2-digermacyclobutanes, and, depending on the substituents, proceeds with a very low or zero barrier. The higher level computation with the 6-311G(d,p) basis set at HF and density functional B3LYP levels of theory confirms this conclusion for the case of dimerization of germenes **1**−**4**; however, they lead to an opposite ruling when the dimerization of 2-fluoro-substituted germene **5** is under investigation. Since the calculation data on dimerization dynamics at the levels of theory higher than HF/3-21G are not yet available for the series of similarly substituted silenes, a comparison of these data with those for germenes can be done so far only at this low level of theory. This comparison shows that the earlier[10] calculated 3-21G barriers for similarly substituted silenes are notably higher than those calculated for germenes in the present work. Therefore, we conclude that within the limits of this level of computation the dimerization of germenes proceeds somewhat easier than dimerization of their silicon analogues. This conclusion is in agreement with our experimental data[11] on dimerization of **3** in the gas phase and in a low-temperature argon or krypton matrixes.

Acknowledgment. Acknowledgment. The support of this work, in part, by the Robert A. Welch Foundation, by Mar Chem, Inc., by U.S. Army Research Office Grant No. DAAH04-96-1-0307, and a grant for supercomputer time from the Houston Advanced Research Center are greatly appreciated. The authors thank the reviewer for valuable comments on the manuscript.

References and Notes

(1) (a) Baines, K. M.; Stibbs, W. G. *Adv. Organomet. Chem.* **1996**, *39*, 275. (b) Escudie, J.; Couret, C.; Ranaivonjatovo, H.; Satge, J. *Coord. Chem. Revs*. **1994**, *130*, 427. (c) Barrau, J.; Escudie, J.; Satge, J. *Chem. Rev.* **1990**, *90*, 283.

(2) (a) Trinquier, G.; Barthelat, J.-C.; Satge, J. *J. Am. Chem. Soc*. **1982**, *104*, 5931. (b) Nagase, S.; Kudo, T. *Organometallics* **1984**, *3*, 324. (c) Grev, R. S.; Schaefer, H. F. *Organometallics* **1992**, *11*, 3489.

(3) (a) Raabe, G.; Michl, J. *Chem. Rev.* **1985**, *85*, 419. (b) Raabe, G.; Michl, J. In *The Chemistry of Organic Silicon Compounds*; Patai, S., Rappoport, Z., Eds.; Wiley and Sons, Ltd.: New York, 1989; Vol. 2, p 1015. (c) Nefedov, O. M. *J. Pure Appl. Chem.* **1991**, *63*, 231.

(4) (a) Apeloig, Y. *Theoretical Aspects of Organosilicon Compounds*; In *The Chemistry of Organic Silicon Compounds*; Patai, S., Rappoport, Z., Eds.; Wiley and Sons, Ltd.: New York, 1989; Vol. 1, Chapter 2, pp 57−225 and references therein. (b) Grev, R. S. *Adv. Organomet. Chem.* **1991**, *33*, 125.

(5) Ahlrichs, R.; Heinzmann, R. *J. Am. Chem. Soc.* **1977**, *99*, 7452.

(6) Morokuma, K.; Kato, S.; Kitaura, K.; Obara, S.; Ohta, K.; Hanamura, S. In *New Horizons of Quantum Chemistry*; Lowdin, P.-O., Pullman, R., Eds.; D. Reidel: Dordrecht, Holland, 1983; pp 221−241.

(7) Apeloig, Y.; Karni, M. *J. Am. Chem. Soc.* **1984**, *106*, 6676.

(8) Seidl, E. T.; Grev, R. S.; Schaefer, H. F. *J. Am. Chem. Soc.* **1992**, *114*, 3643.

(9) (a) Bernardi, F.; Bottoni, A.; Olivucci, M.; Robb, M. A.; Venturini, A. *J. Am. Chem. Soc.* **1993**, *115*, 3322. (b) Bernardi, F.; Bottoni, A.; Olivucci, M.; Venturini, A.; Robb, M. A. *J. Chem. Soc., Faraday Trans.* **1994**, *90* (*12*), 1617−1630.

(10) Morokuma, K. In *Organosilicon and Bioorganosilicon Chemistry: Structure, Bonding, Reactivity and Synthetic Application*; Sakurai, H., Ed.; Ellis Horwood Publ.: Chichester, 1985; Chapter 4, p 37.

(11) (a) Kudin, K. N.; Margrave, J. L.; Khabashesku, V. N. Ninth Summer Research Colloquium, Rice Quantum Institute, August 18, 1995; Abstracts, p 26. (b) Khabashesku, V. N. Fargo Conference on Main Group Chemistry, Fargo, ND, May 30−June 1, 1996; Abstr. O-22. (c) Khabashesku, V. N. Invited Lecture at the 2nd International Conference on Low-Temperature Chemistry, 1996, Kansas City, MO, Aug. 4−9, Proceedings, p 137−140. (d) Khabashesku, V. N.; Kudin, K.; Tamas, J.; Boganov, S. E.; Margrave, J. L.; Nefedov, O. M. *J. Am. Chem. Soc.*, submitted.

(12) *Gaussian 94*. Frisch, M. J.; Trucks, G. W.; Schlegel, H. B.; Gill, P. M. W.; Johnson, B. G.; Robb, M. A.; Cheeseman, J. R.; Keith, T. A.; Petterson, G. A.; Montgomery, J. A.; Raghavachari, K.; Al-Laham, M. A.; Zakrzewski, V. G.; Ortiz, J. V.; Foresman, J. B.; Cioslowski, J.; Stefanov, B. B.; Nanayakkara, A.; Challacombe, M.; Peng, C. Y.; Ayala, P. Y.; Chen, W.; Wong, M. W.; Andres, J. L.; Replogle, E. S.; Gomperts, R.; Martin, R. L.; Fox, D. J.; Binkley, J. S.; Defrees, D. J.; Baker, J.; Stewart, J. P.; Head-Gordon, M.; Gonzalez, C.; Pople, J. A. Gaussian, Inc.: Pittsburgh, PA, 1995.

(13) *Modern Density Functional Theory: A Tool for Chemistry*; Seminario, J. M., Politzer, P., Eds.; Elsevier: Amsterdam, 1995.

(14) (a) Becke, A. D. *J. Chem. Phys.* **1993**, *98*, 5648. (b) Lee, C.; Yang, W; Parr, R. G. *Phys. Rev. B* **1988**, *37*, 785.

(15) (a) *Xmol. Version 1.3.1*. Minnesota Supercomputer Center, Inc., Minneapolis, MN, 1993. (b) Foresman, J. B.; Frisch, A. E. *Exploring*

Chemistry with Electronic Structure Methods; Gaussian, Inc.: Pittsburgh, PA, 1996; Chapter 4, pp 70−72.

(16) Allouche, A. *REDONG, Vibrational Analysis and Coordinate Transformation of a GAUSSIAN 88 Calculation.* CNRS URA 773, Marseille, France. *QCPE Program N 628*. Department of Chemistry, Indiana University, IN.

(17) Windus, T. L.; Gordon, M. S. J. *Am. Chem. Soc.* **1992**, *114*, 9559.

(18) Wong, N. W. *Chem. Phys. Lett.* **1996**, *256*, 391.

(19) (a) Siebert, H. *Anwendungen der Schwingungsspektroskopie in der Anorganischen Chemie*; Springer-Verlag: Berlin, 1966. (b) Siebert, H. *Z. Anorg. Allg. Chem.* **1953**, *273*, 170.

(20) (a) Brook, A. G.; Harris, J. W.; Lennan, J.; El Sheikh, M. *J. Am. Chem. Soc.* **1979**, *101*, 83. (b) Brook, A. G.; Nyburg, S. C.; Reynolds, W. F.; Poon, Y. C.; Chang, Y.-M.; Lee, J.-S.; Picard, J.-P. *J. Am. Chem. Soc*. **1979**, *101*, 6750. (c) Brook, A. G.; Brook, M. A. *Adv. Organomet. Chem*. **1996**, *39*, 71.